

# Observation of the exclusive decay $B \rightarrow e\nu D^*$ and search for $B \rightarrow e\nu\pi^0$

Crystal Ball Collaboration

D. Antreasyan<sup>8</sup>, H.W. Bartels<sup>4</sup>, C. Bieler<sup>7</sup>, J.K. Bienlein<sup>4</sup>, A. Bizzeti<sup>6</sup>, E.D. Bloom<sup>10</sup>, K. Brockmüller<sup>4</sup>, A. Cartacci<sup>6</sup>, M. Cavalli-Sforza<sup>2</sup>, R. Clare<sup>10</sup>, A. Compagnucci<sup>6</sup>, G. Conforto<sup>6</sup>, S. Cooper<sup>10</sup>, D. Coyne<sup>2</sup>, K. Fairfield<sup>10</sup>, G. Folger<sup>5</sup>, A. Fridman<sup>10,a</sup>, D. Gelfman<sup>10</sup>, G. Glaser<sup>5</sup>, G. Godfrey<sup>10</sup>, K. Graaf<sup>7</sup>, F.H. Heimlich<sup>6,7</sup>, F.H. Heinsius<sup>7</sup>, R. Hofstadter<sup>10</sup>, J. Irion<sup>8</sup>, Z. Jakubowski<sup>3</sup>, H. Janssen<sup>9</sup>, K. Karch<sup>4,11</sup>, S. Keh<sup>11</sup>, T. Kiel<sup>7</sup>, H. Kilian<sup>11</sup>, I. Kirkbride<sup>10</sup>, M. Kobel<sup>5</sup>, W. Koch<sup>4</sup>, A.C. König<sup>9</sup>, K. Königsmann<sup>11,b</sup>, S. Krüger<sup>7</sup>, G. Landi<sup>6</sup>, S. Leffler<sup>10</sup>, R. Lekebusch<sup>7</sup>, T. Lesiak<sup>3</sup>, A.M. Litke<sup>10</sup>, S. Lowe<sup>10</sup>, B. Lurz<sup>5</sup>, H. Marsiske<sup>4,10</sup>, W. Maschmann<sup>4,7</sup>, P. McBride<sup>8</sup>, W.J. Metzger<sup>9</sup>, H. Meyer<sup>4</sup>, B. Monteleoni<sup>6</sup>, B. Muryn<sup>3,c</sup>, B. Niczyporuk<sup>10</sup>, G. Nowak<sup>3</sup>, C. Peck<sup>1</sup>, P.G. Pelfer<sup>6</sup>, F.C. Porter<sup>1</sup>, M. Reidenbach<sup>9</sup>, M. Scheer<sup>11</sup>, P. Schmitt<sup>11</sup>, J. Schotanus<sup>9</sup>, J. Schütte<sup>5</sup>, A. Schwarz<sup>10</sup>, D. Sievers<sup>7</sup>, T. Skwarnicki<sup>4</sup>, V. Stock<sup>7</sup>, K. Strauch<sup>8</sup>, U. Strohbush<sup>7</sup>, J. Tompkins<sup>10</sup>, B. van Uitert<sup>10</sup>, R.T. Van de Walle<sup>9</sup>, A. Voigt<sup>4</sup>, U. Volland<sup>5</sup>, K. Wachs<sup>4</sup>, K. Wacker<sup>10</sup>, W. Walk<sup>9</sup>, H. Wegener<sup>5</sup>, D.A. Williams<sup>8,2</sup>

<sup>1</sup> California Institute of Technology<sup>d</sup>, Pasadena, CA 91125, USA

<sup>2</sup> University of California at Santa Cruz<sup>e</sup>, Santa Cruz, CA 95064, USA

<sup>3</sup> Cracow Institute of Nuclear Physics, PL-30055 Cracow, Poland

<sup>4</sup> Deutsches Elektronen Synchrotron DESY, D-2000 Hamburg, Federal Republic of Germany

<sup>5</sup> Universität Erlangen-Nürnberg<sup>f</sup>, D-8520 Erlangen, Federal Republic of Germany

<sup>6</sup> INFN and University of Firenze, I-50125 Firenze, Italy

<sup>7</sup> Universität Hamburg, I. Institut für Experimentalphysik<sup>g</sup>, D-2000 Hamburg, Federal Republic of Germany

<sup>8</sup> Harvard University<sup>h</sup>, Cambridge, MA 02138, USA

<sup>9</sup> University of Nijmegen and NIKHEF<sup>i</sup>, NL-6525 ED Nijmegen, The Netherlands

<sup>10</sup> Department of Physics<sup>k</sup>, HEPL, and Stanford Linear Accelerator Center<sup>l</sup>, Stanford University, Stanford, CA 94305, USA

<sup>11</sup> Universität Würzburg<sup>m</sup>, D-8700 Würzburg, Federal Republic of Germany

Received 4 May 1990

**Abstract.** The Crystal Ball detector at the  $e^+e^-$  storage ring DORIS II has been used to analyze exclusive semileptonic decays of  $B$  mesons produced at  $\Upsilon(4S)$  energies. The decay  $B \rightarrow e\nu D^*$  has been observed with a branching ratio of  $(7.0 \pm 1.8 \pm 1.4)\%$  using the  $\pi^0 D$  decay mode of the  $D^*$ . In addition we have searched for the exclusive semileptonic decay  $B^\pm \rightarrow e^\pm \nu \pi^0$ . We find an upper limit on  $\text{BR}(B^\pm \rightarrow e^\pm \nu \pi^0)$  of 0.22% at the 90% CL.

<sup>a</sup> Permanent address: DPHPE, Centre d'Etudes Nucléaires de Saclay, F-91191 Gif sur Yvette, France

<sup>b</sup> Permanent address: CERN, CH-1211 Genève 23, Switzerland

<sup>c</sup> Permanent address: Institute of Physics and Nuclear Techniques, AGH, PL-30055 Cracow, Poland

<sup>d</sup> Supported by the U.S. Department of Energy, contract No. DE-AC03-81ER40050 and by the National Science Foundation, grant No. PHY75-22980

<sup>e</sup> Supported by the National Science Foundation, grant No. PHY85-12145

<sup>f</sup> Supported by the German Bundesministerium für Forschung und Technologie, contract No. 054 ER 12P(5)

<sup>g</sup> Supported by the German Bundesministerium für Forschung und Technologie, contract No. 054 HH 11P(7) and by the Deutsche Forschungsgemeinschaft

<sup>h</sup> Supported by the U.S. Department of Energy, contract No. DE-AC02-76ER03064

## 1 Introduction

Measuring the elements of the Cabibbo-Kobayashi-Maskawa quark mixing matrix [1] in weak decays is an important task in particle physics since the values of these elements are fundamental parameters of the standard model. In a previous paper [2] we have analyzed the inclusive electron spectrum from  $B$  meson decays to charmed final states, resulting in a determination of  $|V_{cb}|$ . Theoretically one expects [3–8] the electron spectrum to be dominated by the final states  $e\nu D$  and  $e\nu D^*$ , contributing approximately 30% and 60% to the total width. A determination of the individual contributions may help to distinguish between different theoretical models.

Inclusive semileptonic  $B$  decays to *non-charm* final states have been studied to extract  $|V_{ub}|$ . In the beginning

<sup>i</sup> Supported by FOM-ZWO

<sup>k</sup> Supported by the U.S. Department of Energy, contract No. DE-AC03-76SF00326 and by the National Science Foundation, grant No. PHY81-07396

<sup>l</sup> Supported by the U.S. Department of Energy, contract No. DE-AC03-76SF00515

<sup>m</sup> Supported by the German Bundesministerium für Forschung und Technologie, contract No. 054 WU 11P(1)

only upper limits could be derived [2, 9]. Recently both CLEO [10] and ARGUS [11] reported signals from  $b \rightarrow u$  transitions in inclusive semileptonic decays resulting in a value [11] of  $|V_{ub}|/|V_{cb}| \simeq 0.10$ .

To determine  $|V_{ub}|$  from an experimental measurement, e.g., the branching ratio of semileptonic  $b \rightarrow u$  transitions, the hadronic matrix element between the initial state  $B$  meson and the final state meson has to be known. While calculations of the  $b \rightarrow c$  hadronic matrix element with different models give reasonable agreement for the inclusive decay rate, the predictions for inclusive  $b \rightarrow u$  transitions are much more model dependent [3–8]. More reliable results for  $|V_{ub}|$  may come from measurements of *exclusive* semileptonic  $B$  meson decays [12–15].

In this article we present two analyses of exclusive semileptonic  $B$  meson decays. The paper is organized as follows: Section 2 gives a short introduction to the experimental setup. In Sect. 3 the observation and analysis of the decay  $B \rightarrow e\nu D^*$ ,  $D^* \rightarrow \pi^0 D$  is reported. The search for  $B^\pm \rightarrow e^\pm \nu \pi^0$  is presented in Sect. 4. Finally we summarize our results on exclusive  $B$  decays.

## 2 Experimental setup

A detailed description of the Crystal Ball detector at the DORIS II electron-positron storage ring at DESY has been given elsewhere [2]. It is a non-magnetic calorimetric detector consisting of 672 NaI(Tl) crystals of 16 radiation lengths thickness, covering 93% of the full solid angle. The solid angle coverage is increased to 98% of  $4\pi$  sr by NaI(Tl) endcap crystals. Four double layers of chambers containing in total 800 drift tubes are used to detect charged particles and to measure their directions. For the present analysis the detector's ability to identify and to measure the energy and direction of electrons and photons from 10 MeV upwards is important. The energy resolution for electrons and photons is given

by  $\sigma_E/E = (2.7 \pm 0.2)\% / \sqrt{E/\text{GeV}}$ ; their directions are measured with an accuracy in the polar angle  $\vartheta$  with respect to the beam axis of  $\sigma_\vartheta = 1^\circ$  to  $3^\circ$ , where the resolution is best for high-energy showers.

Neutral pions are reconstructed from their decay into two photons. For  $\pi^0$  energies below about 500 MeV, these two photons are well separated in the calorimeter. For more energetic  $\pi^0$  mesons the showers of the two photons can overlap in the calorimeter forming only one cluster. At energies above 1.5 GeV  $\pi^0$  candidates are selected by analyzing the moments of the shower patterns of neutral energy clusters [16].

## 3 Observation of the decay $B \rightarrow e\nu D^* \rightarrow e\nu\pi^0 D$

We identify the semileptonic  $B$  meson decay chain

$$B \rightarrow e\nu D^* \rightarrow e\nu\pi^0 D \quad (1)$$

by a high-energy electron back-to-back with a slow  $\pi^0$ . Near the electron endpoint energy, the neutrino has low energy and momentum. The semileptonic  $B$  decay then

resembles a two-body decay  $B \rightarrow eD^*$  with the  $D^*$  recoiling against the electron in the  $B$  rest frame. The  $D^*$  has a sizeable branching ratio for the decay  $D^* \rightarrow \pi^0 D$ . Due to the small mass difference,  $M_{D^*} - M_D \approx 140$  MeV, the emitted  $\pi^0$  has low momentum in the  $D^*$  rest frame ( $p_{\pi^0} \approx 40$  MeV/c). Boosted by the  $D^*$  motion, the  $\pi^0$  preserves approximately the  $D^*$  direction. The pion is not monochromatic, but still soft ( $p_{\pi^0} \leq 250$  MeV/c) in the laboratory frame. The observation of a soft  $\pi^0$  recoiling back-to-back with a high energy electron therefore identifies the decay chain (1). The event sample selected in this way includes both charged and neutral  $B$  meson decays.

There are four effects which lead to an opening angle less than  $180^\circ$  between the directions of the electron and the  $\pi^0$ :

- The momentum carried away by the neutrino. Since the electron spectrum decreases rapidly towards the endpoint one has to compromise between event statistics and the requirement that the electron and slow pion be back-to-back.
- The boost resulting from the non-zero momentum of the  $B$  mesons ( $p_B \approx 340$  MeV/c) produced in the reaction

$$e^+ e^- \rightarrow \Upsilon(4S) \rightarrow B\bar{B}. \quad (2)$$

- The transverse  $\pi^0$  momentum relative to the  $D^*$  direction.
- The angular resolution of the detector.

Background arises from  $\pi^0$ 's produced by the decays of the  $D$  meson in reaction (1), by decays from the second  $B$  meson in reaction (2) and from semileptonic  $B\bar{B}$  decays to  $D$  mesons.

### 3.1 Data preselection

The Crystal Ball data used in this analysis were taken on the  $\Upsilon(4S)$  resonance, with most of the data (90%) accumulated on the top of the resonance. The integrated luminosity is  $92 \text{ pb}^{-1}$ . This corresponds to  $N_B = (140.0 \pm 2.8) \times 10^3$  produced  $B$  mesons [2], where the error is dominated by the luminosity measurement. For background studies,  $30 \text{ pb}^{-1}$  of data have been taken in the continuum just below the  $\Upsilon(4S)$  resonance.

Hadronic events are first selected by criteria which are the same as those applied in our inclusive analysis of the electron spectrum [2]. Then we strengthen the multiplicity and topology cuts as follows. Events originating from  $\Upsilon(4S)$  resonance decays are enhanced compared to those from hadronic continuum production by requiring a high multiplicity, i.e., at least 8 local energy maxima in the calorimeter, and non-jetlike events by a cut on the second Fox-Wolfman moment [17]:

$$H_2 \equiv \frac{\sum_i \sum_j E_i E_j (3 \cos^2 \alpha_{ij} - 1)}{2(\sum_k E_k)^2} < 0.40. \quad (3)$$

The  $E_{i,j}$  denote the deposited energies assigned to single particles and the  $\alpha_{ij}$  are the angles between these energy

deposits. While resonance events are selected with high efficiency, these cuts suppress background from the continuum process  $e^+e^- \rightarrow q\bar{q}$ . The remaining continuum contribution is subtracted using continuum data to which the same event selection criteria have been applied.

### 3.2 Particle identification and reconstruction

Energy depositions which lie within  $|\cos\vartheta| < 0.85$  and which are identified as charged by the proportional chambers are treated as electron candidates. The lateral pattern of their energy deposition in the NaI is required to be consistent with that expected for a single electromagnetically showering particle. The continuum-subtracted electron spectrum in  $\Upsilon(4S)$  decays for these identified electrons is displayed in Fig. 1.

Our analysis uses only electrons with energy  $E_e$  in the range  $1800 \text{ MeV} \leq E_e \leq 2300 \text{ MeV}$ . The stringent lower cut on the electron energy ensures that the neutrino in the semileptonic  $B$  decay is soft. Also  $B$  decays to other charmed mesons heavier than the  $D^*$  are suppressed. After continuum subtraction the sample contains  $N_e = (1256 \pm 61)$  electrons from semileptonic  $B$  decays.

This electron sample was checked for two different sources of background, neither of which contributes significantly. The continuum-subtracted distribution of pulse heights in the drift tubes agrees with that for electrons and allows only a negligibly small contribution from pions [2]. The second source of background could originate from converted decay photons of fast  $\pi^0$ 's yielding a single energy cluster similar to those from electrons. This background is estimated by reanalyzing the data with the same cuts as for electrons, but taking neutral energy clusters instead of clusters tagged as electrons. The continuum subtracted result is scaled down by the conversion probability for the two photons from  $\pi^0$  decays ( $2 \times 5\% = 10\%$ ). We find that only 2 background events contribute to the sample of 1256 electrons.

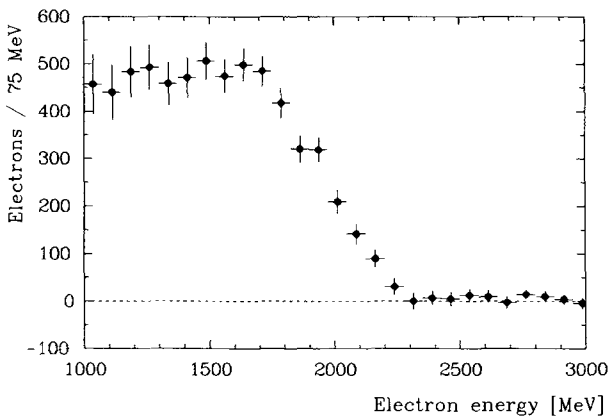


**Fig. 1.** The inclusive electron spectrum in  $\Upsilon(4S)$  decays. Continuum contributions have been subtracted bin by bin

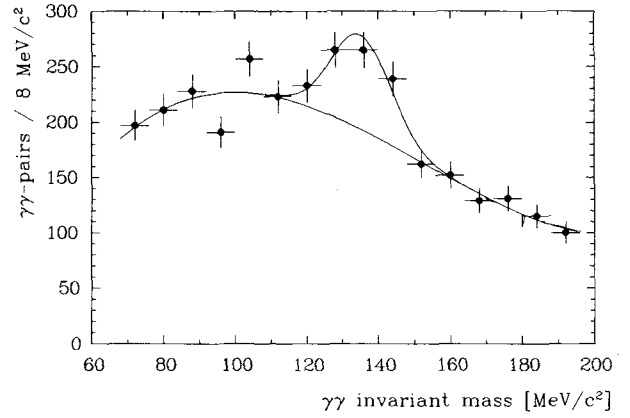


**Fig. 2.** The invariant mass distribution of all two-photon combinations after the cuts on  $p_{\pi^0}$  and  $E_\gamma$  as given in the text. Superimposed on the data is a fit with a line shape for the  $\pi^0$  signal (cf. Sect. 3.3) and a polynomial background

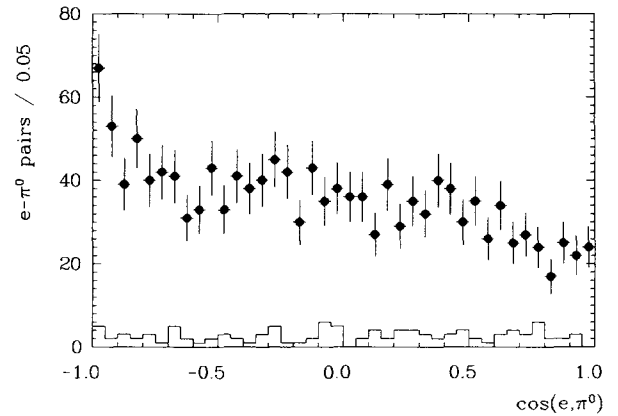


**Fig. 3.** This distribution of the cosine of the angle between the electron and the  $\pi^0$  (data points) for the  $\Upsilon(4S)$  resonance data and the continuum data below the  $\Upsilon(4S)$  (histogram). The integrated luminosities are  $92 \text{ pb}^{-1}$  and  $30 \text{ pb}^{-1}$ , respectively. The  $B \rightarrow e\nu D^*$ ,  $D^* \rightarrow \pi^0 D$  events peak at  $\cos(e, \pi^0) = -1$

Slow  $\pi^0$  mesons are reconstructed through the invariant mass of the two photons from their decay. The lateral shower distribution of the photons in the calorimeter is required to be consistent with that of single electromagnetically showering particles. Next we require the  $\pi^0$  momentum  $p_{\pi^0}$  to be in the range  $30 \text{ MeV}/c < p_{\pi^0} < 240 \text{ MeV}/c$  and the energies  $E_\gamma$  of both decay photons to satisfy  $30 \text{ MeV} < E_\gamma < 190 \text{ MeV}$ . The efficiency of these cuts is above 90% for  $\pi^0$  mesons produced in the decay (1). However, these cuts reduce the contamination from other processes substantially. The distribution of the invariant mass of the two-photon combinations is plotted in Fig. 2. A  $\pi^0$  signal on a combinatoric background is visible.

Since we aim to tag the  $D^*$  mesons through the  $e-\pi^0$  angular correlation, we have to investigate the distribution of the cosine of the angle between the electron and the  $\pi^0$ ,  $\cos(e, \pi^0)$ . The distribution of  $\cos(e, \pi^0)$  for all  $\gamma\gamma$ -combinations with  $110 \text{ MeV} < m_{\gamma\gamma} < 160 \text{ MeV}$  is

shown in Fig. 3. The  $\cos(e, \pi^0)$  distribution for the continuum data taken just below the  $\Upsilon(4S)$  resonance is also displayed in Fig. 3 as a histogram. The luminosity ratio between the resonance and the continuum sample is about 3:1. Only in the resonance sample do we observe an enhancement of  $e-\pi^0$  pairs at  $\cos(e, \pi^0) \approx -1$ . We attribute this structure to  $B \rightarrow e\nu D^*$  decays.

### 3.3 Background subtraction

Most of the background visible under the  $D^*$  signal in Fig. 3 is due to combinatoric background under the  $\pi^0$  peak in the  $M_{\gamma\gamma}$  distribution (see Fig. 2). We parametrize this background  $N_{bg}$  as a two-dimensional function of  $\cos(e, \pi^0)$  and  $M_{\gamma\gamma}$  in the form

$$\frac{d^2 N_{bg}}{d \cos(e, \pi^0) d M_{\gamma\gamma}} = \sum_{i=0}^2 \sum_{j=0}^3 a_{ij} C_i(\cos(e, \pi^0)) C_j(\hat{M}_{\gamma\gamma}), \quad (4)$$

where  $C_i, C_j$  are Chebyshev polynomials and  $\hat{M}_{\gamma\gamma} = 2\{(M_{\gamma\gamma} - M_{\gamma\gamma}^{\min}) / (M_{\gamma\gamma}^{\max} - M_{\gamma\gamma}^{\min})\} - 1$ . Thus the  $\cos(e, \pi^0)$ -dependence is described by a quadratic polynomial and the  $M_{\gamma\gamma}$ -dependence by a cubic polynomial.

The line shape of the  $\pi^0$  signal,  $L(M_{\gamma\gamma})$ , was studied with a Monte Carlo simulation of the reaction chain  $B \rightarrow e\nu D^*, D^* \rightarrow \pi^0 D$ . It was found that the  $\pi^0$  shape is well represented by a Gaussian with width  $\sigma_{\pi^0} = (8.5 \pm 0.3)$  MeV/ $c^2$ , modified at low and high  $M_{\gamma\gamma}$  values by power law tails. The lower-mass tail just reflects the asymmetric photon line shape in the Crystal Ball calorimeter [18], while the higher-mass tail results from the overlap of photons with other energy depositions in high multiplicity  $\Upsilon(4S)$  events. This line shape was then fitted with a  $\cos(e, \pi^0)$ -dependent amplitude  $dN_{\pi^0}/d \cos(e, \pi^0)$  on top of the background described above:

$$\frac{d^2 N}{d \cos(e, \pi^0) d M_{\gamma\gamma}} = \frac{dN_{\pi^0}}{d \cos(e, \pi^0)} \frac{dL}{d M_{\gamma\gamma}} + \frac{d^2 N_{bg}}{d \cos(e, \pi^0) d M_{\gamma\gamma}}. \quad (5)$$

This function is fitted by the maximum likelihood method to the observed two-dimensional distribution (14 bins of varying bin size in  $\cos(e, \pi^0)$  and 19 bins in  $M_{\gamma\gamma}$  of width 8 MeV). The  $dN_{\pi^0}/d \cos(e, \pi^0)$  distribution resulting from the fit is plotted in Fig. 4.

There is still some background in this distribution which we attribute to  $\pi^0$ 's not originating from  $D^*$  decays. This background was investigated with the help of a Monte Carlo and was found to be flat over the full  $\cos(e, \pi^0)$  range. We thus fit the distribution in Fig. 4 in the full range of  $\cos(e, \pi^0)$  by a flat background and a contribution from  $B \rightarrow e\nu D^*$  events. The shape of the latter distribution is taken from the Monte Carlo simulation described in the following section and is shown as the histogram in Fig. 4. We find  $N_{e\pi^0} = (71 \pm 18)$  events, where  $N_{e\pi^0}$  is the number of observed  $B \rightarrow e\nu D^*, D^* \rightarrow \pi^0 D$  events. The total number of random  $e-\pi^0$  pairs,

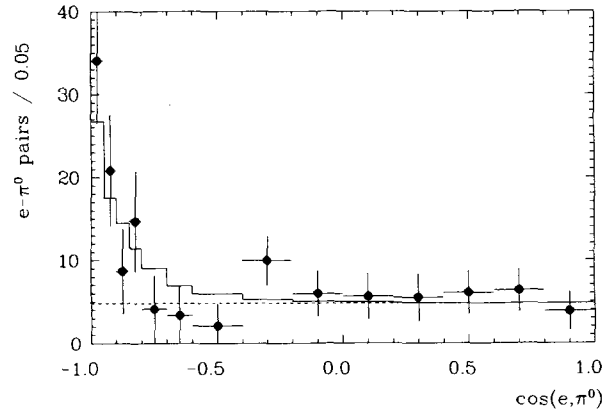


**Fig. 4.** The distribution of the cosine of the angle between the electron and the  $\pi^0$  (data points) after background subtraction of fake  $\pi^0$ 's. A fit of the  $B \rightarrow e\nu D^*, D^* \rightarrow \pi^0 D$  contribution (histogram) plus a flat background (dashed line) from uncorrelated  $e-\pi^0$  pairs is shown. The shape of the  $\cos(e, \pi^0)$  distribution for  $B \rightarrow e\nu D^*$  events is obtained by a Monte Carlo simulation based on the model in [3]

distributed uniformly over  $\cos(e, \pi^0)$ , is 193. Systematic effects in the estimation of  $N_{e\pi^0}$  were studied by

- changing the binning of the data and varying fit ranges ( $\pm 13\%$ ),
- replacing the  $\pi^0$  line shape by a simple Gaussian ( $\pm 6\%$ ),
- using different theoretical models [3, 4, 19] for the prediction of the  $\cos(e, \pi^0)$  distribution ( $\pm 7\%$ ).

Adding these individual relative errors in quadrature, we obtain a total systematic error on  $N_{e\pi^0}$  of  $\pm 16\%$ .

### 3.4 Detection efficiencies

The detection efficiencies were estimated using Monte Carlo techniques. With the Lund string fragmentation program version 6.2 [20], we simulated the decay chain:

$$\Upsilon(4S) \rightarrow B\bar{B}, \quad B_1 \rightarrow e\nu D^* \rightarrow e\nu\pi^0 D; \quad B_2 \rightarrow \text{anything}. \quad (6)$$

The energy and angular distributions in the decay of the first  $B$  meson were taken from the predictions of Grinstein et al. [3]. Decays of the  $D$  meson and of the other  $B$  meson were performed by the standard Lund Monte Carlo [20] with updated  $B, D$  and  $D_s$  meson branching ratios [21]. The generated events were then passed through a complete detector simulation and subjected to the same cuts as described above.

The electron selection efficiency as determined by Monte Carlo is  $\varepsilon_e = (13.1 \pm 0.7)\%$ . This efficiency includes the hadronic event selection (90%), the geometrical acceptance (85%), the electron identification in the chambers and in the calorimeter (54%) and the efficiency of our electron energy cut (32%). The 5% systematic error on  $\varepsilon_e$  [2] does not include the uncertainty due to the cut on the electron energy. The efficiency of this cut depends on the theoretical input for the shape of

the electron spectrum in  $B \rightarrow e\nu D^*$  decays. For example, using the model of Wirbel et al. [4] instead of the model of Grinstein et al. [3], changes our efficiency by  $\Delta\varepsilon_e/\varepsilon_e = -6.5\%$ .

The reconstruction efficiency for a  $\pi^0$  in events containing an identified electron is  $\varepsilon_{\pi^0} = (13.6 \pm 0.7)\%$ . The error is dominated by the uncertainties in modeling photon conversions and by accidental tagging due to random chamber hits.

### 3.5 Results and discussion

The branching ratio for the decay  $B \rightarrow e\nu D^*$  is obtained from

$$\text{BR}(B \rightarrow e\nu D^*) = \frac{N_{e\pi^0}}{N_B \langle \text{BR}(D^* \rightarrow \pi^0 D) \rangle \varepsilon_e \varepsilon_{\pi^0}}, \quad (7)$$

where  $\langle \text{BR}(D^* \rightarrow \pi^0 D) \rangle$  denotes the branching ratio for  $D^* \rightarrow \pi^0 D$  transitions averaged over the different charge states of  $D^*$  mesons produced in  $\Upsilon(4S)$  decays according to (1) and (2). This quantity can be written as  $\langle \text{BR}(D^* \rightarrow \pi^0 D) \rangle = \omega \text{BR}^0 + (1 - \omega) \text{BR}^+$  with

$$\omega = \frac{\text{BR}(\Upsilon(4S) \rightarrow B^+ B^-)}{\text{BR}(\Upsilon(4S) \rightarrow B^+ B^-) + \text{BR}(\Upsilon(4S) \rightarrow B^0 \bar{B}^0)} \quad (8)$$

and  $\text{BR}^+ = \text{BR}(D^{*\pm} \rightarrow \pi^0 D^\pm)$ ,  $\text{BR}^0 = \text{BR}(D^{*0} \rightarrow \pi^0 D^0)$ . For the branching ratios  $\text{BR}^+$  and  $\text{BR}^0$  we use weighted means of the world averages [21] and the new MARK III measurements [22]. This yields  $\text{BR}^+ = (27 \pm 3)\%$  and  $\text{BR}^0 = (55 \pm 6)\%$ . The ratio  $\omega$  has not yet been measured. We follow standard practice [24, 26] and assume  $\omega = 0.5$ .

With the above branching ratios we obtain the following result:

$$\text{BR}(B \rightarrow e\nu D^*) = (7.0 \pm 1.8 \pm 1.4)\%$$

where the first error is statistical and the second error includes in quadrature all systematic errors in  $N_{e\pi^0}$  and  $N_B$ ,  $\text{BR}^+$  and  $\text{BR}^0$ ,  $\varepsilon_e$  and  $\varepsilon_{\pi^0}$ . This branching ratio refers to a mixture of  $B$  mesons.

Our measurement is complemented by ARGUS [23] and CLEO [24] measurements of  $B^0 \rightarrow l^\pm \nu D^{*\mp}$ , in which the decay of the  $D^{*\mp}$  was fully reconstructed. They obtained  $(5.4 \pm 0.9 \pm 1.3)\%$  (ARGUS) and  $(4.6 \pm 0.5 \pm 0.7)\%$  (CLEO). Using an average of these measurements and the result from our analysis, we estimate the branching ratio  $\text{BR}(B^\pm \rightarrow e^\pm \nu D^{*0})$  and obtain

$$\text{BR}(B^\pm \rightarrow e^\pm \nu D^{*0}) = (8.0 \pm 3.4)\%.$$

Assuming equal leptonic widths for  $B^\pm$  and  $B^0$  mesons the lifetime ratio for  $B$  mesons is given by  $\tau(B^\pm)/\tau(B^0) = \text{BR}(B^\pm \rightarrow e^\pm \nu D^{*0})/\text{BR}(B^0 \rightarrow e^\pm \nu D^{*\mp})$ . Inserting the above given numbers yields

$$\tau(B^\pm)/\tau(B^0) = (1.7 \pm 0.8).$$

The lifetime ratio agrees with that obtained by ARGUS [25] from a comparison of the yields of  $\bar{D}^0$ ,  $D^-$  and

$D^{*-}$  in semileptonic  $B$  decays:  $\tau(B^\pm)/\tau(B^0) = (1.00 \pm 0.27)$ .

We cannot exclude the possibility of additional sources of soft pions contributing to the  $B$  decay signal seen in our analysis, e.g.,  $B \rightarrow e\nu D^* \pi$ , where the  $D^* \pi$  may include a  $D^{**}$  resonance contribution. ARGUS finds no evidence for such decays [23], whereas CLEO's fit to their data is somewhat improved by a contribution of  $(14 \pm 8)\%$  from such decays [24]. Theoretically, semileptonic  $B$  decays to bound states heavier than  $D^*$  are expected to be essentially negligible after our electron energy cut ( $E_e > 1800$  MeV) [3]. In any case, this cut acts to reduce the contribution from any hadronic state, resonant or not, heavier than the  $D^*$ . For example, we have estimated that even if  $\text{BR}(B \rightarrow e\nu D^{**}(2420))$  is as high as 20% of  $\text{BR}(B \rightarrow e\nu D^*)$ , it would contribute less than 7% to our signal.

## 4 Search for the decay $B^\pm \rightarrow e^\pm \nu \pi^0$

Much effort has been put into searches for exclusive  $b \rightarrow u$  transitions which allow a direct measurement of the CKM matrix element  $|V_{ub}|$ . Most of the searches have been performed using hadronic decay modes of the  $B$  mesons. We have searched for the semileptonic channel

$$B^\pm \rightarrow e^\pm \nu \pi^0 \quad (9)$$

by measuring the missing mass of the  $e\pi^0$  system. This can be expressed as:

$$M_\nu^2 = (E_\nu)^2 - (\mathbf{p}_\nu)^2 = (E_{\text{beam}} - E_e - E_{\pi^0})^2 - (\mathbf{p}_B - \mathbf{p}_e - \mathbf{p}_{\pi^0})^2. \quad (10)$$

The beam energy  $E_{\text{beam}}$  is known to a sufficient precision and the momentum of the  $B$  mesons produced on the  $\Upsilon(4S)$  resonance is negligible ( $p_B \approx 340$  MeV/c) so that the reconstruction of an electron together with a high energy  $\pi^0$  leads to the identification of channel (9).

### 4.1 Data analysis

A major subset of the sample used in the analysis described in the preceding section has been analyzed. The integrated luminosity of this subsample taken on the  $\Upsilon(4S)$  resonance amounts to  $76 \text{ pb}^{-1}$ , corresponding to  $N_B = (128.4 \pm 2.6) \times 10^3$  produced  $B$  mesons. The data sample as well as the hadronic event selection criteria are identical to those used in our analysis of the inclusive electron spectrum [2]. A continuum sample of  $18.5 \text{ pb}^{-1}$  integrated luminosity is used for background studies.

The suppression of continuum hadron production compared to resonance production is achieved by the following cuts (see Sect. 3.1):  $H_2 < 0.50$  and the number of local energy maxima  $\geq 8$ . Due to smaller expected background, the cut on  $H_2$  is chosen softer than that in the previous analysis. The electron candidates are required to fulfill criteria similar to those imposed in our

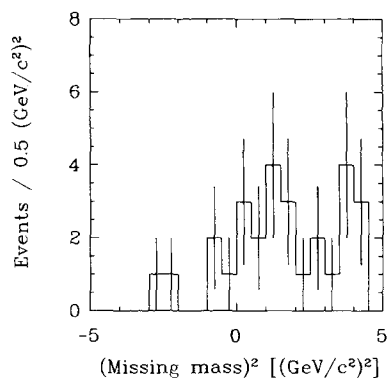


**Fig. 5.** The squared missing mass to the electron and the  $\pi^0$  for  $B$  decays in  $Y(4S)$  data

analysis of the decay  $B \rightarrow e\nu D^*$ . High energy  $\pi^0$  mesons are identified as neutral energy clusters in the calorimeter. The second moment of the shower distribution of these neutral clusters has to be consistent with that expected for high energy neutral pions. We use only electrons and pions with energies between 1500 MeV to 2600 MeV. A reduction of combinatoric background with the decay products of the other  $B$  meson is achieved by requiring  $\cos(e, \pi^0)$  to be less than  $-0.5$ . The resulting missing mass spectrum is plotted in Fig. 5. There remain  $(28 \pm 5)$  events in the range  $-5 \text{ GeV}^2/c^4$  to  $+5 \text{ GeV}^2/c^4$ . From continuum data we expect  $(8 \pm 6)$  continuum events in the same missing mass range after scaling by the ratio of luminosities and squared beam energies. The residual  $(20 \pm 8)$  events can be assigned to  $B$  decays.

Background studies have been done using a Monte Carlo simulation. A sample of  $61 \times 10^3$   $Y(4S) \rightarrow B\bar{B}$  decays, simulating the decay chain

$$Y(4S) \rightarrow B\bar{B}, \quad B_1 \rightarrow e\nu X_c, \quad B_2 \rightarrow \text{anything}, \quad (11)$$

has been subjected to the analysis described above. Here  $X_c$  denotes a charmed meson state. After scaling to the produced  $B\bar{B}$  events we obtain  $(14 \pm 4)$  background events from this sample in the missing mass range given above. Thus only  $(6 \pm 9)$  events remain as possible  $B \rightarrow e\nu\pi^0$  decays. Since the above-mentioned background contributions have large statistical and systematic errors we chose to determine an upper limit on the branching ratio of the decay  $\text{BR}(B^\pm \rightarrow e^\pm \nu\pi^0)$  by a fit to the unsubtracted spectrum of Fig. 5.

#### 4.2 Upper limit determination and discussion

The detection efficiency  $\varepsilon$  has been determined using a Monte Carlo simulation of the decay searched for:

$$Y(4S) \rightarrow B\bar{B}, \quad B_1 \rightarrow e\nu\pi^0; \quad B_2 \rightarrow \text{anything}. \quad (12)$$

The missing mass spectrum for this data sample is shown in Fig. 6, where the normalization corresponds to the number of events expected in our event sample for a

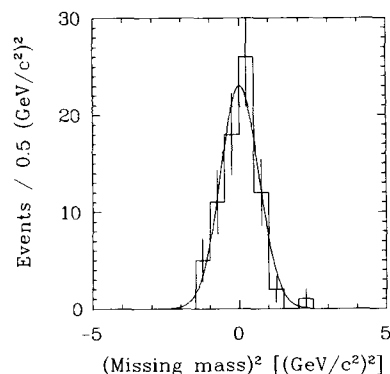


**Fig. 6.** The squared missing mass to the electron and the  $\pi^0$  for Monte Carlo data. The Gaussian fit to this spectrum yields the position and width to be used in the fit to the  $Y(4S)$  events

branching ratio of  $\text{BR}(B^\pm \rightarrow e^\pm \nu\pi^0) = 3\%$ . The detection efficiency is calculated from a Gaussian fit to this spectrum, see Fig. 6. We obtain  $\varepsilon = (3.9 \pm 0.5)\%$ , where statistical and a systematic error of  $\pm 7\%$  (5% each from  $\varepsilon_e$  and  $\varepsilon_{\pi^0}$ , see Sect. 3.4) have been added in quadrature.

To determine the upper limit we fit the unsubtracted spectrum of Fig. 5 with a Gaussian signal of position and width derived from the Monte Carlo and a linear function to account for background. A series of maximum likelihood fits to the unbinned spectrum is performed with the signal amplitude fixed for each fit. This yields the likelihood as a function of the signal strength. Integrating the likelihood from 0 to 90% of its area yields 5.4 events at the 90% confidence level.

To obtain the upper limit for the branching ratio  $\text{BR}(B^\pm \rightarrow e^\pm \nu\pi^0) = N/(\omega N_B \varepsilon)$  we must include the experimental errors. We convolute the above likelihood function with a Gaussian centered at  $\omega N_B \varepsilon$  and with a width obtained by adding in quadrature the errors  $\sigma_{N_B} = 2\%$  and  $\sigma_\varepsilon = 13\%$ . We obtain a 90% confidence level upper limit of

$$\text{BR}(B^\pm \rightarrow e^\pm \nu\pi^0) < 0.22\%.$$

For decays of *neutral*  $B$  mesons the ARGUS group [26] has obtained  $\text{BR}(\bar{B}^0 \rightarrow l^- \nu\pi^+) < 0.09\%$ .

As discussed in the introduction, a measurement of this channel gives a constraint on the CKM matrix element  $|V_{ub}|$ . Using a factorization approach, Wirbel et al. [4] predict a partial width  $\Gamma(B^\pm \rightarrow e^\pm \nu\pi^0) = 7.9 \times 10^{12} |V_{ub}|^2 \text{ s}^{-1}$ . With  $\text{BR}(B^\pm \rightarrow e^\pm \nu\pi^0) = \Gamma(B^\pm \rightarrow e^\pm \nu\pi^0) \times \tau_B$  and the world average value for the  $B$  meson life time [21],  $\tau_B = (1.31^{+0.14}_{-0.13}) \times 10^{-12} \text{ s}$  we obtain the following limit on the CKM matrix element:

$$|V_{ub}| < 0.015. \quad (13)$$

This result is comparable with limits obtained from other exclusive searches for semileptonic  $b \rightarrow u$  transitions [26, 27]. For example, ARGUS' limit on the decay  $\text{BR}(\bar{B}^0 \rightarrow l^- \nu\pi^+)$  yields together with the model by Wirbel et al. a limit  $|V_{ub}| < 0.009$ . In addition we can deduce a limit on the ratio  $|V_{ub}|/|V_{cb}|$  with our measurement of

$|V_{cb}| = 0.055 \pm 0.005$  from an analysis of the inclusive electron spectrum [2] using the same model of Wirbel et al. We obtain:

$$|V_{ub}|/|V_{cb}| < 0.27 \text{ at the 90\% CL.}$$

This value is consistent with  $|V_{ub}|/|V_{cb}| \simeq 0.10$  deduced from the recently reported signals [10, 11] in inclusive semileptonic  $b \rightarrow u$  transitions.

As the value of  $|V_{ub}|$  is now known [10, 11] one can turn the argument around and deduce an upper limit on the hadronic matrix element (usually given by  $\tilde{F}$ , defined by  $\Gamma_{\text{partial}} = \tilde{F} \times |V_{ub}|^2 \times 10^{-11}$  GeV). We find

$$\tilde{F} < 5.3$$

which has to be compared with model calculations of  $\tilde{F} = 0.53$  by [4] and a range of 0.0110 to 0.239 as compiled and evaluated by [28]. So the experimental data samples have to be enlarged considerably to be able to measure the important decay channel  $B^\pm \rightarrow \pi^0 e^\pm \nu$ . One has to be aware that the result for  $\tilde{F}$  is not an independent measurement as for the evaluation of  $|V_{ub}|$  from the measurement of the inclusive electron spectrum the same theoretical models have to be used, see [28].

## 5 Conclusions

The Crystal Ball group has analyzed exclusive  $B$  decay channels containing electrons and  $\pi^0$  mesons. In particular the decay  $B \rightarrow e\nu D^* \rightarrow e\nu\pi^0 D$  has been observed for a mixture of  $B^\pm$  and  $B^0$  mesons with a branching ratio (using the model of Grinstein et al.) of  $(7.0 \pm 1.8 \pm 1.4)\%$ . Together with measurements of the branching ratio  $\text{BR}(B^0 \rightarrow l^\pm \nu D^{*\mp})$  we obtain a first measurement of the semileptonic decay of charged  $B^\pm$  mesons using the neutral pion decay of  $D^{*0}$  mesons:  $\text{BR}(B^\pm \rightarrow e^\pm \nu D^{*0}) = (8.0 \pm 3.4)\%$ .

A search for exclusive charmless  $B$  decays has been made by investigating the missing mass spectrum of the  $e\pi^0$  system in the decay  $B^\pm \rightarrow e^\pm \nu \pi^0$ . We obtain a 90% confidence level upper limit of 0.22% on the branching ratio. This results in a 90% CL upper limit  $|V_{ub}| < 0.015$  using the hadronic matrix element predictions of Wirbel et al. Combined with our analysis of the inclusive electron spectrum, we obtain an upper limit of 0.27 for  $|V_{ub}|/|V_{cb}|$ . Turning the argument around and using the recent value for  $|V_{ub}|$  we get an upper limit to the square of the hadronic matrix element of  $\tilde{F} < 5.3$ .

*Acknowledgments.* We would like to thank the DESY and SLAC directorates for their support. This experiment would not have been possible without the dedication of the DORIS machine group as well as the experimental support groups at DESY. The visiting groups thank the DESY laboratory for the hospitality extended to them. Z.J., B.Mu., B.N., and G.N. thank DESY for financial support. E.D.B., R.H., and K.S. have benefited from financial support from the Humboldt Foundation. K. Königsmann acknowledges support from a Heisenberg fellowship.

## References

1. N. Cabibbo: Phys. Rev. Lett. 10 (1963) 531; M. Kobayashi, T. Maskawa: Prog. Theor. Phys. 49 (1973) 652
2. K. Wachs et al.: Z. Phys. C – Particles and Fields 42 (1989) 33; K. Wachs: Ph. D. Thesis, University of Hamburg, DESY-F31-88-01 (1988), unpublished
3. B. Grinstein, N. Isgur, D. Scora, M.B. Wise: Phys. Rev. D 39 (1989) 799; B. Grinstein, M.B. Wise, N. Isgur: Phys. Rev. Lett. 56 (1986) 298
4. M. Wirbel, B. Stech, M. Bauer: Z. Phys. C – Particles and Fields 29 (1985) 637
5. S. Nussinov, W. Wetzel: Phys. Rev. D 36 (1987) 130
6. J.M. Cline, W.F. Palmer, G. Kramer: Phys. Rev. D 40 (1989) 793
7. C.A. Dominguez, N. Paver: Z. Phys. C – Particles and Fields 41 (1988) 217
8. M. Suzuki: Phys. Rev. D 37 (1988) 239
9. H. Albrecht et al.: Phys. Lett. B 209 (1988) 119; S. Behrends et al.: Phys. Rev. Lett. 59 (1987) 407; T. Jensen et al.: Nucl. Phys. B (Proc. Suppl.) 1 (1988) 91; C. Klopfenstein et al.: Phys. Lett. B 130 (1983) 444
10. R. Fulton et al.: Phys. Rev. Lett. 64 (1990) 16
11. H. Albrecht et al.: Phys. Lett. B 234 (1990) 409
12. B. Grinstein, M.B. Wise: Phys. Lett. B 197 (1987) 249
13. T. Altomari, L. Wolfenstein: Phys. Rev. D 37 (1988) 681
14. K. Hagiwara, A.D. Martin, M.F. Wade: DTP/89/12 (1989)
15. J.G. Körner, G.A. Schuler: Phys. Lett. B 226 (1989) 185
16. P. Schmitt et al.: Z. Phys. C – Particles and Fields 40 (1988) 199
17. G.C. Fox, S. Wolfram: Phys. Rev. Lett. 41 (1978) 1581; *ibid.*: Nucl. Phys. B 149 (1979) 413
18. J. Gaiser et al.: Phys. Rev. D 34 (1986) 711
19. S.C. Chao et al.: Phys. Rev. D 31 (1985) 1756
20. T. Sjöstrand: Comput. Phys. Commun. 39 (1986) 347; T. Sjöstrand, M. Bengtsson: Comput. Phys. Commun. 43 (1987) 367
21. Particle Data Group: Phys. Lett. 204 B (1988) 1
22. J. Adler et al.: Phys. Lett. 208 B (1988) 152
23. H. Albrecht et al.: Phys. Lett. 197 B (1987) 452; the branching ratio quoted here was obtained by scaling to  $\omega=0.5$ , see M. Danilov [26]
24. D. Bortoletto et al.: Phys. Rev. Lett. 63 (1989) 1667
25. H. Albrecht et al.: Phys. Lett. 232 B (1989) 554
26. H. Albrecht et al.: DESY 89-163 (1989); M. Danilov in: Proc. of the Int. Lepton Photon Symp., Stanford 1989
27. D. Bortoletto et al.: Phys. Rev. Lett. 62 (1989) 2436
28. G. Kramer, W.F. Palmer: DESY 90-011 (1990)